CHAPTER II

LITERATURE REVIEW

2.1 Introduction

The Photovoltaic (PV) was discovered by Bell Labs researchers in 1954 [1]. These PV solar cells were first used by the U.S in the late 1950's to power space satellites. After its success in space, PV was manufactured on a commercial scale to power small electronic devices, such as solar powered calculators.

Countries along equator can benefit from strong solar energy about 4-6.9 kilowatt-hours per square meter per day shown in figure 2.1 [2]. Therefore, solar photovoltaic attracts a lot of attention in this tropical region. Today, with improvements in technology and manufacturing methods, PV is a rapidly emerging renewable energy technology for residential and large-scale commercial applications.

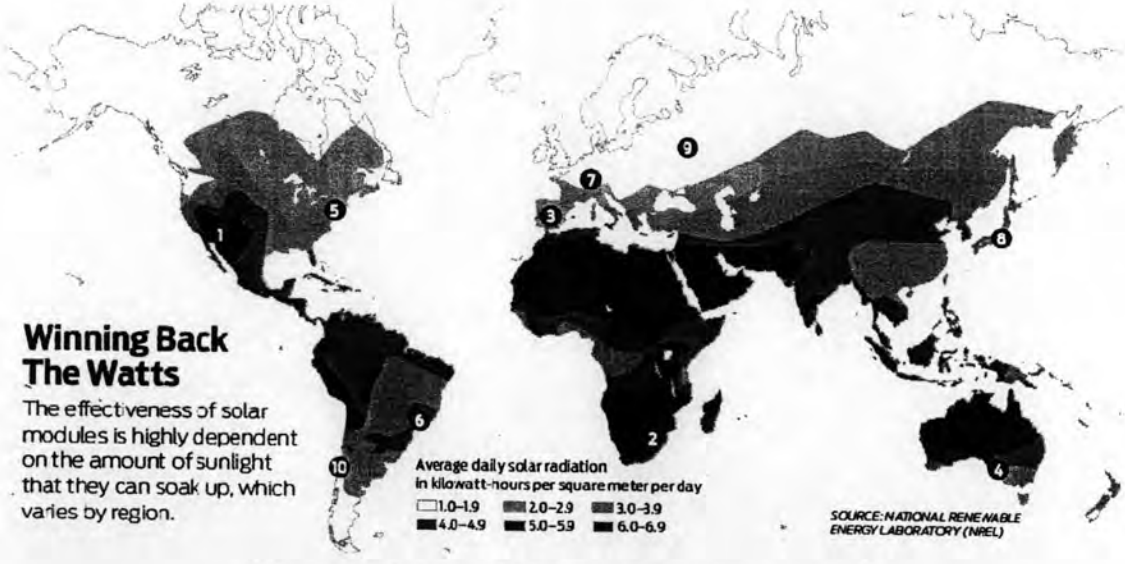

Figure 2-1 Average daily solar radiation in kW/h/m^2

2.2 Photovoltaic Cell [3]

Photovoltaic cells are made of special materials called semiconductors such as silicon, which is currently the most commonly used. Basically, when light strikes the cell, a certain portion of it is absorbed within the semiconductor material. This means that the energy of the absorbed light is transferred to the semiconductor. The energy

knocks electrons loose, allowing them to flow freely. PV cells also all have one or more electric fields that act to force electrons freed by light absorption to flow in a certain direction. This flow of electrons is a current, and it can draw that current off to use externally by placing metal contacts on the top and bottom of the PV cell. Silicon happens to be a very shiny material, which means that it is very reflective. Photons that are reflected cannot be used by the cell. Therefore, the basic structure of photovoltaic shown in figure 2-2 should contain: A is the glass cover plate that protects the cell from the elements; B is antireflective coating that is applied to the top of the cell to reduce reflection losses to less than 5 percent. C and F are contact grid, and back contact, use for current flow; D and E are N-type and P-type silicon.

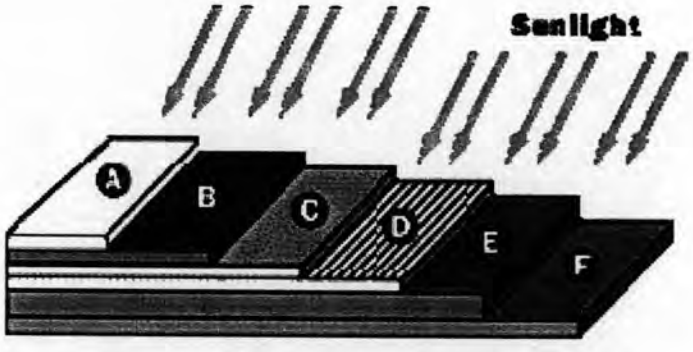

Figure 2-2 Basic structure of silicon PV Cell

2.2.1 Semiconductor Physics

Silicon has some special chemical properties, especially in its crystalline form. An atom of silicon has 14 electrons in figure 2-3.a [3], arranged in three different shells, and convenient shorthand is drawn in figure 2-3.b [3]. The first two shells, those closest to the center, are completely full. The outer shell, however, is only half full, having only four electrons. A silicon atom will always look for ways to fill up its last shell (which would like to have eight electrons). To do this, it will share electrons with four of its neighbor silicon atoms. It is like every atom holds hands with its neighbors, except that in this case, each atom has four hands joined to four neighbors. That is what forms the crystalline structure, and that structure turns out to be important to this type of PV.

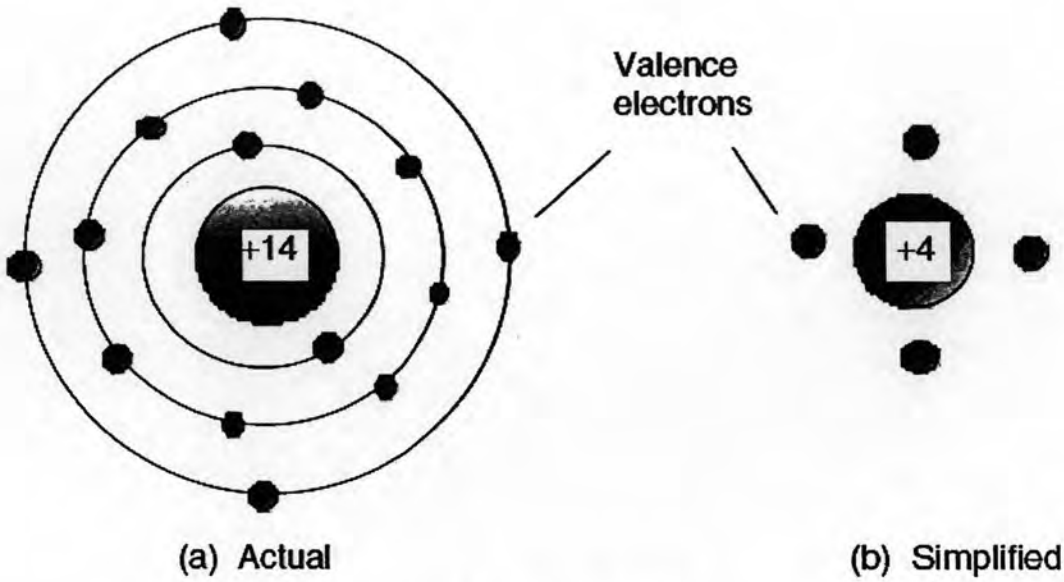

Figure 2-3 Physics of Silicon

PV cells have two types of semi-conductors shown in figure 2-4: n-type and p-type. The n-type semi-conductor is made up of silicon and phosphorus, while the p-type is comprised of silicon and boron. The n-type and p-type semi-conducting materials are placed together, creating a p-n junction. When sunlight comes into contact with the solar cell, the atoms in the n-type semiconductors become "excited," causing the free electrons in the n-type semiconductor to move towards the p-type semiconductor and fill the "hole" caused by the missing electron. This flow of electrons creates an electric current, shown in figure 2-5. This is called the "photovoltaic effect."

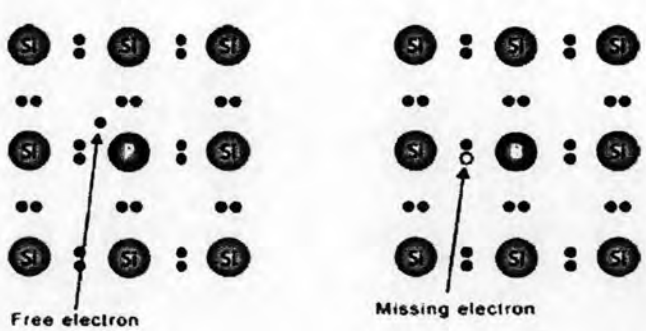

Figure 2-4 N-Type Semiconductor, Silicon (Si) doped with Phosphorus (P), and P-Type Semiconductor, Silicon (Si) doped with Boron (B)

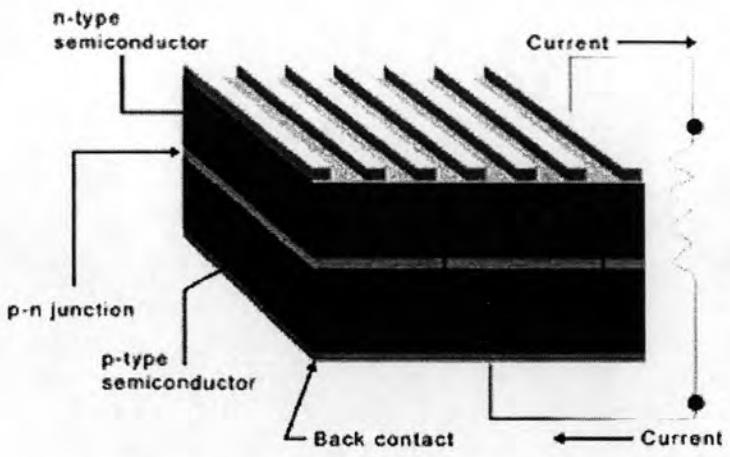

Figure 2-5 Electrical current created by the electron flowing

2.2.2 Photovoltaic Characteristic

According to figure 2-5, a simple equivalent circuit model for a photovoltaic cell consists of a real diode in parallel with an ideal current source shown in figure 2-6 [3]. The two actual PV characteristics are the current that flows when the terminals are shorted together (the short-circuit current, I_{sc}), and the voltage across the terminals when the leads are left open (the open-circuit voltage, V_{OC}).

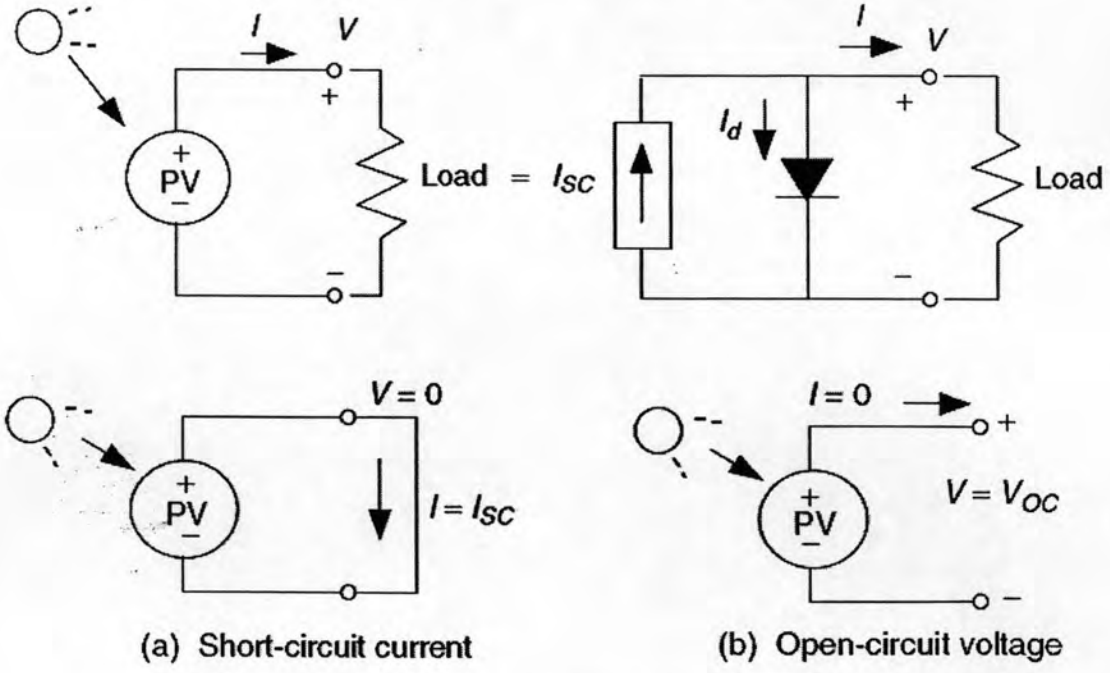

Figure 2-6 Simple equivalent circuit for PV cell

The characteristic of I_{sc} and V_{oc} can be derived as:

$$I = I_{sc} - I_d \tag{2-1}$$

$$I_d = I_0(e^{q\frac{V_d}{nkT}} - 1) \tag{2-2}$$

$$I = I_{sc} - I_0(e^{q\frac{V_d}{nkT}} - 1) \tag{2-3}$$

where I_{sc} : Photocurrent, function of irradiation level and junction temperature (A)

I : Cell output current (A)

I_0 : Reverse saturation current of diode (A)

V_d : diode voltage (V)

q: Electron charge (Coulomb)

k : Boltzmann constant (J/°K)

n : Diode quality factor, it takes a value between 1 and 2

In short circuit condition, terminal voltage of PV cell will equal zero. So, I is equal to I_{sc}. In contrary, I equals zero in open circuit condition. Therefore, the open circuit voltage, V_{oc} can derive as:

$$V_{oc} = \frac{nkT}{q}\ln(\frac{I_{sc}}{I_0} + 1) \tag{2-4}$$

It is interesting to note that the second term in the equation 2-1 is just the diode equation with a negative sign. So its characteristic curve is just I_{sc} added to the diode curve turned upside-down, where curve of current–voltage relationship for a PV cell for no sunlight "dark", and for an illuminated cell "light" shown in figure 2-7 [3]. The dark curve is just the diode curve turned upside-down. The light curve is the dark curve plus I_{sc}.

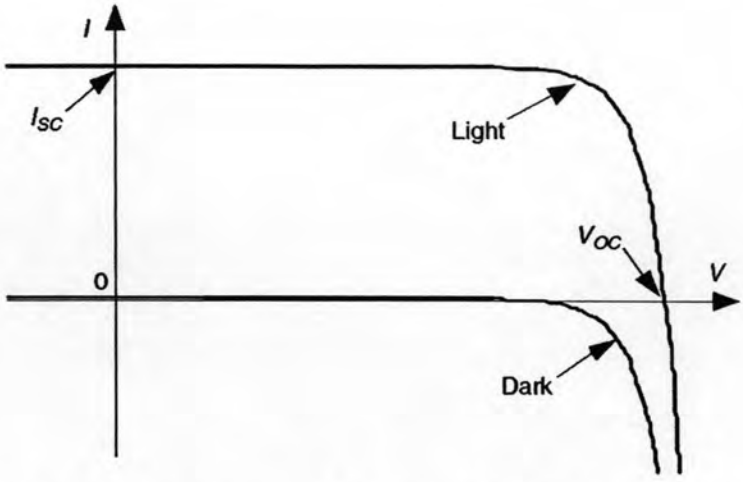

Figure 2-7 Curve of current–voltage relationship for a PV cell

The PV cells are wired in series or string to form a PV module. In this case, the shaded cell could happen if any cell in that string is in the dark. Therefore, to improve the accuracy of PV cell equivalent circuit, the parallel or series resistance is added into the PV cell equation shown in figure 2-8 [3]. Where the modification of PV equivalent circuit by adding parallel resistance,R_p can cause the current at any given voltage to drop by V/R_p shown in figure 2-9 [3]. Where the adding series resistance, R_s can cause the voltage at any given current shifted to the left by $\Delta V = IR_s$ shown in figure 2-10 [3].

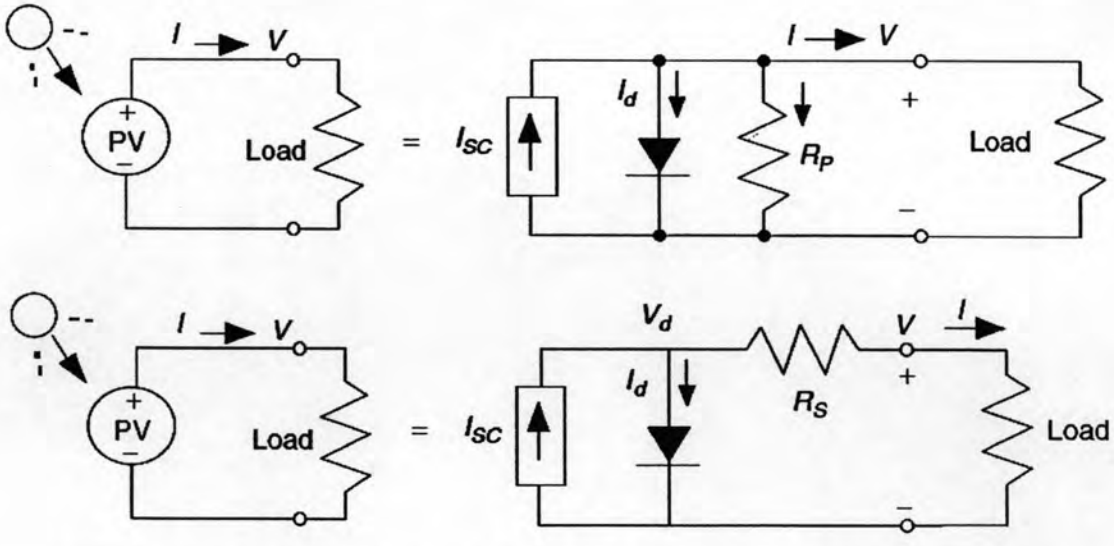

Figure 2-8 Modification of PV equivalent circuit by adding parallel or series resistance

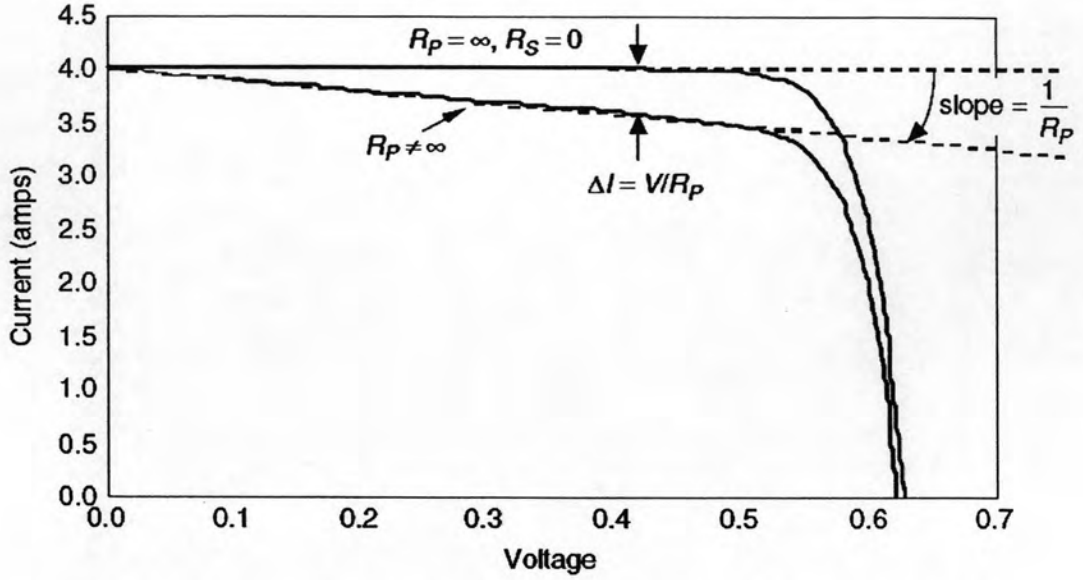

Figure 2-9 Curve of I-V characteristic of a PV cell by adding parallel resistance

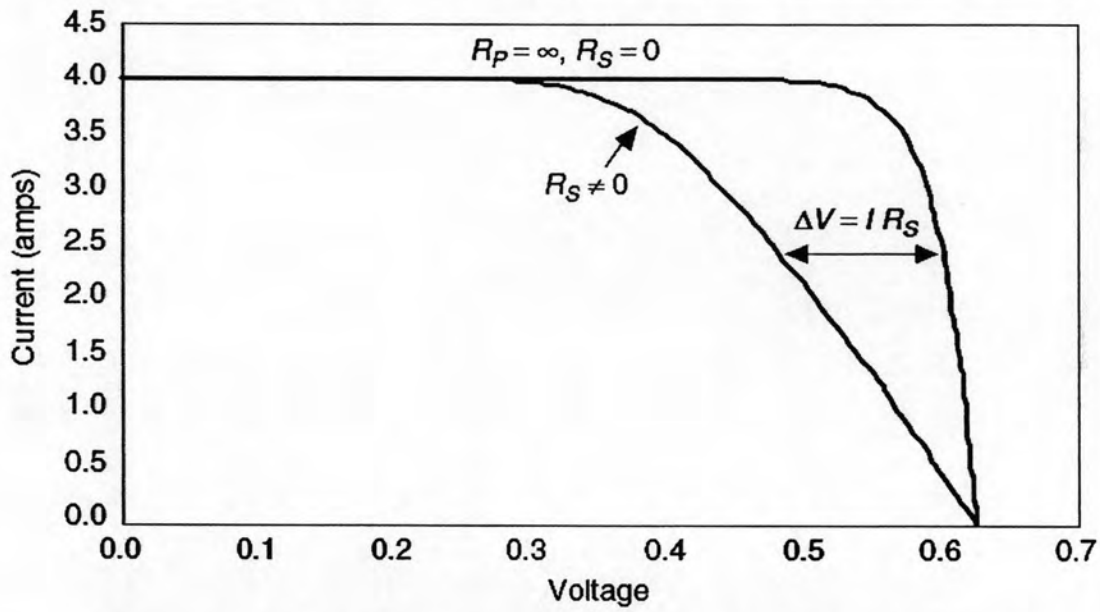

Figure 2-10 Curve of I-V characteristic of a PV cell by adding series resistance

According to figure 2-8, the equation 2-1 by adding parallel resistance can derive as:

$$I = I_{sc} - I_0(e^{q\frac{V_d}{nkT}} - 1) - \frac{V}{R_p} \qquad \textbf{(2-5)}$$

And the modification of equation 2-1 by adding series resistance can also derive as:

$$I = I_{sc} - I_0(e^{q\frac{V + I.R_s}{nkT}} - 1) \qquad \textbf{(2-6)}$$

2.2.3 Photovoltaic Module and Array

Replying to the voltage and current requirement in the application system, the PV cells are wired in series to increase the voltage and parallel to increase the current shown in figure 2-11 [3]. The combination of PV cell in series and parallels is called PV module, and the combination of PV module in series and parallels is called array shown in figure 2-12 [3].

To avoid the shading problem in the PV array, the bypass diode is adding in parallel with each module. In practice, it may not practical to add bypass diodes across every solar cell. Instead, manufacturers may provide at least one bypass diode around a module to help protect arrays or several such diodes around groups of cells within a module. These diodes do not have much impact on shading problems of a single module, but they can be very important when a number of modules are connected in series shown in figure 2-13 [3].

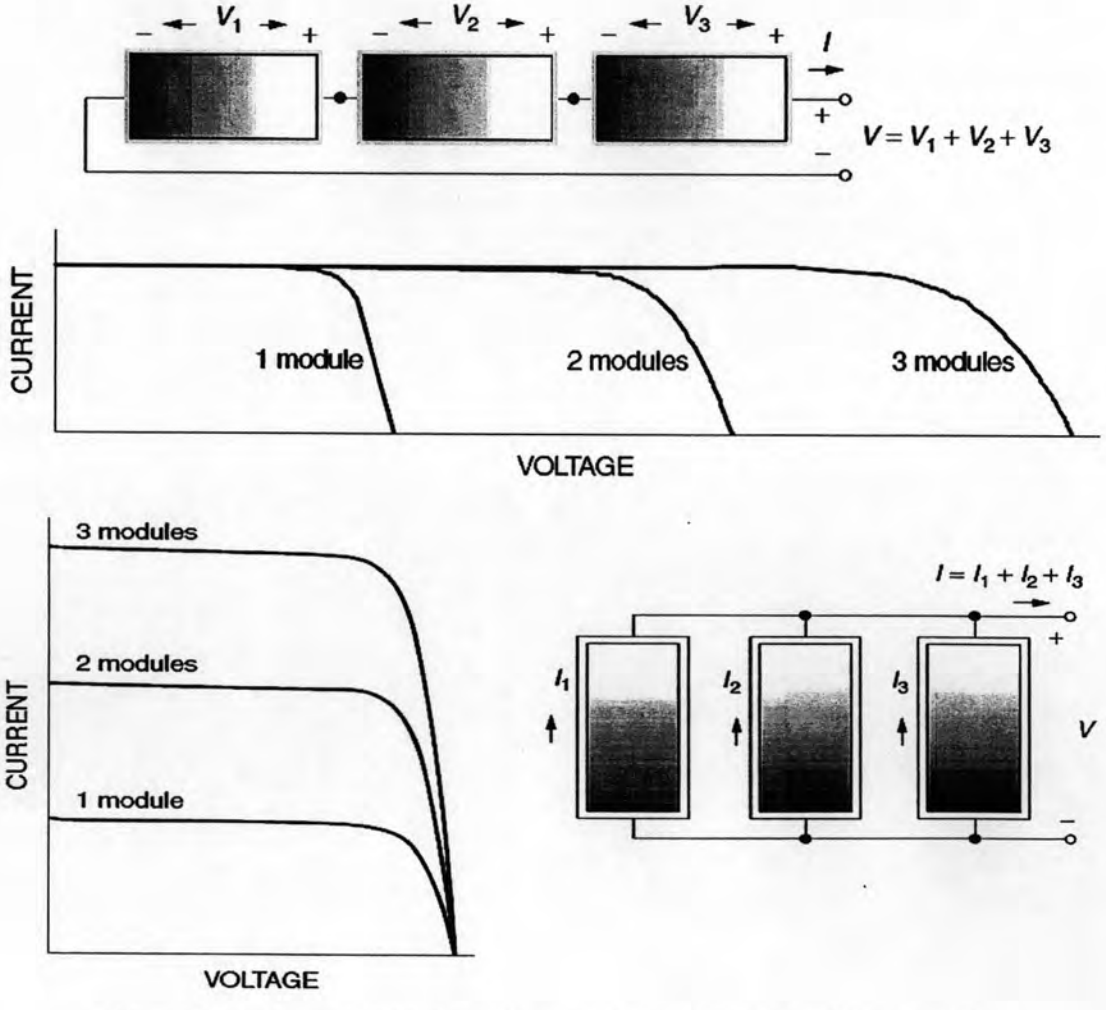

Figure 2-11 Curve of I-V characteristic by wiring in series and in parallels

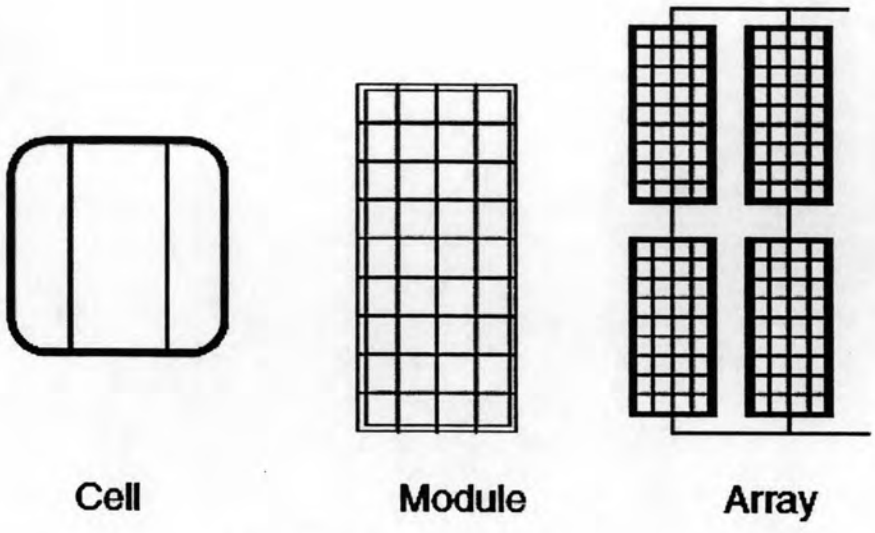

Figure 2-12 PV cell, module, and array

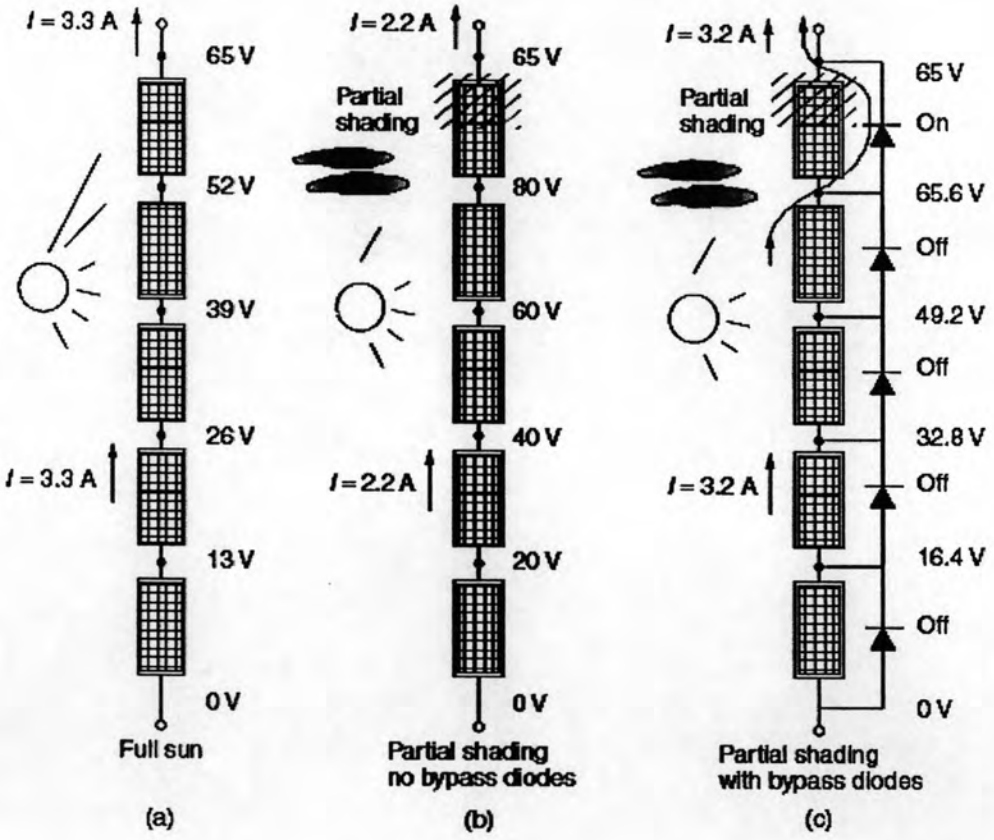

Figure 2-13 Shading with and without bypass diodes

2.3 Grid-Connected Photovoltaic Systems

Generally, the GCPV systems contain the PV array shown in section 2.2, boost converter circuit to achieve higher voltage, maximum power point tracking (MPPT) technique to track the maximum output power from the PV array, and PWM inverter with voltage regulator.

2.3.1 Boost Converter [4]

PV system often stacks modules in series to achieve higher voltage. However, sufficient stacking of modules is not possible in many high voltage applications due to lack of space. Therefore, boost converters shown in figure 2-14 [4] is used to increase the voltage and reduce the number of modules in series. It is a class of switching-mode power supply (SMPS) containing at least two semiconductor switches (a diode and a transistor) and at least one energy storage element. Filters made of capacitors (sometimes in combination with inductors) are normally added to the output of the converter to reduce output voltage ripple.

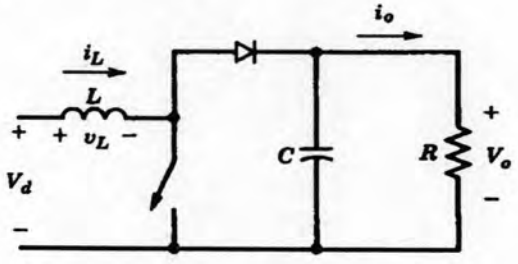

Figure 2-14 Boost converter diagram

In continuous mode, the inductor current (I_L) never falls to zero. Figure 2-15 [4] shows the typical waveforms of currents and voltages in a converter operating in this mode. The output voltage can be calculated as follows, in the case of an ideal converter operating in steady conditions.

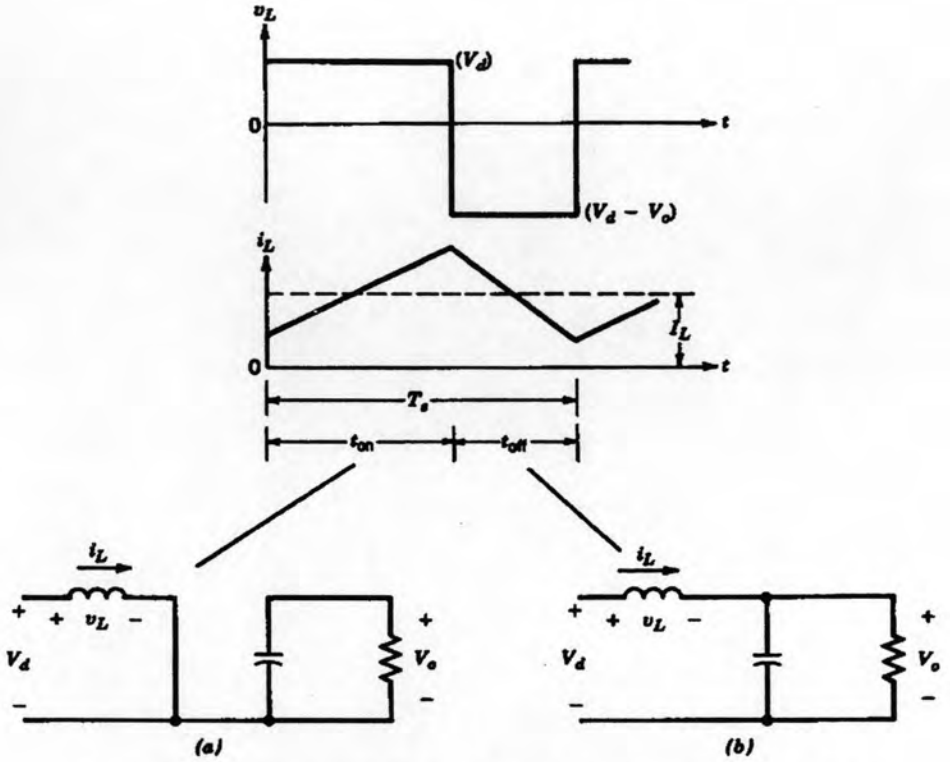

Figure 2-15 Continuous-conduction mode: (a) On-state, (b) Off-state

During the On-state, the switch S is closed shown in figure 2-15.a, which makes the input voltage (V_d) appear across the inductor, which causes a change in current (I_L) flowing through the inductor during a time period (t) can be derived as:

$$\frac{\Delta I_L}{\Delta t} = \frac{V_d}{L} \tag{2-7}$$

At the end of the On-state, the increase of I_L is:

$$\Delta I_{L_{On}} = \frac{1}{L}\int_0^{DT} V_d dt = \frac{DTV_d}{L} \tag{2-8}$$

During the Off-state, the switch S is opened shown in figure 2-15.b, so the inductor current flows through the load. If we consider zero voltage drops in the diode, and a capacitor large enough for its voltage to remain constant, the evolution of I_L is:

$$V_d - V_0 = L\frac{dI_L}{dt} \tag{2-9}$$

Therefore, the variation of I_L during the Off-state is:

$$\Delta I_{L_{off}} = \int_0^{(1-D)T} \frac{(V_d - V_0)}{L} dt = \frac{(V_d - V_0)(1-D)T}{L} \tag{2-10}$$

In steady-state conditions, the amount of energy stored in each of its component has to be the same at the beginning and at the end of a commutation cycle. Therefore, the inductor current has to be the same at the beginning and the end of the commutation cycle. This can be written as:

$$\Delta I_{L_{On}} + \Delta I_{L_{Off}} = \frac{V_d DT}{L} + \frac{(V_d - V_0)(1-D)T}{L} = 0 \quad \text{, or} \quad \frac{V_o}{V_d} = \frac{1}{(1-D)} \tag{2-11}$$

and,

$$\frac{I_o}{I_d} = 1 - D \tag{2-12}$$

During the boundary between continuous and discontinuous conduction shown in figure 2-16.a, the inductor current is going to zero at the end of the off interval, where figure 2-16.b is the function of duty ratio varying while the output voltage is constant.

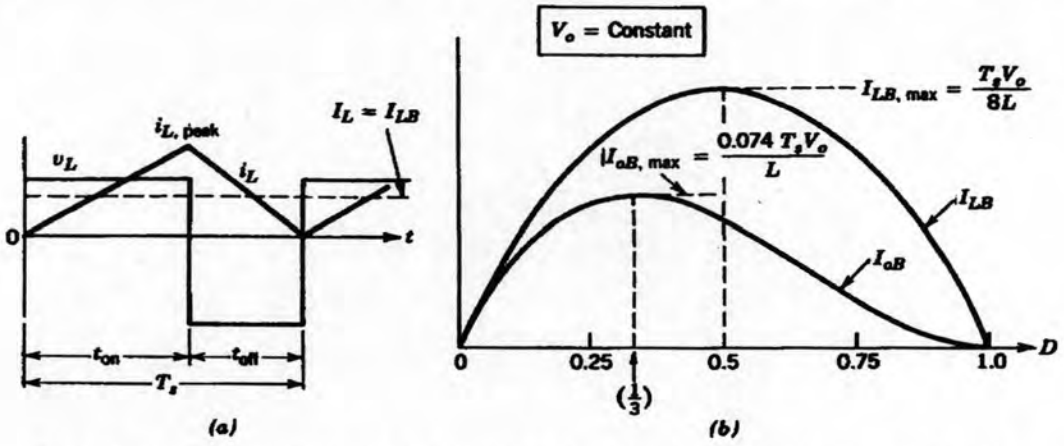

Figure 2-16 Boost converter at the boundary of continuous-discontinuous conduction

Therefore, the average value of the inductor current is:

$$I_{LB} = \frac{T_s V_0}{2L} D(1-D) \tag{2-13}$$

In this condition, the I_d=I_L. So, the average output current at the edge of continuous conduction is:

$$I_{oB} = \frac{T_s V_0}{2L} D(1-D)^2 \tag{2-14}$$

In discontinuous conduction, the amount of energy required by the load is small enough to be transferred in a time smaller than the whole commutation period. In this case, the current through the inductor falls to zero during part of the period. The only

difference in the principle described above is that the inductor is completely discharged at the end of the commutation cycle shown in figure 2-17 [4].

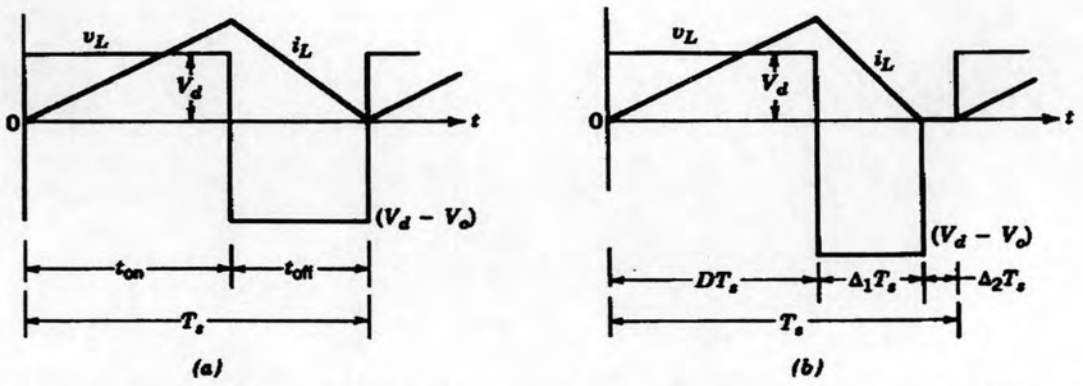

Figure 2-17 Boost converter waveform: (a) at boundary of continuous-discontinuous conduction, (b) at discontinuous conduction

In this case, V_d and D are constants. While the decreased P_o $(=P_d)$, I_L $(=I_d)$, and $I_{L,peak}$ is the same as in boundary at boundary of continuous-discontinuous conduction. Therefore, the inductor voltage over one time period to zero is:

$$\frac{V_o}{V_d} = \frac{\Delta_1 + D}{\Delta_1} \tag{2-15}$$

and,

$$\frac{I_o}{I_d} = \frac{\Delta_1}{\Delta_1 + D} \tag{2-16}$$

The average input current that equals to the inductor current is:

$$I_d = \frac{V_d}{2L} DT_s(D + \Delta_1) \tag{2-17}$$

Using equation 2-12 in the foregoing yields:

$$I_0 = \frac{T_s V_d}{2L} D\Delta_1 \tag{2-18}$$

2.3.2 Maximum Power Point Tracking

The maximum power point tracking (MPPT) of a photovoltaic array is usually an essential part of a PV system to draw peak power from the solar array in order to maximize the produced energy to DC-DC converter. Many MPPT methods have been developed and implemented [5]. The methods vary in complexity, sensors required, convergence speed, cost, range of effectiveness, implementation hardware, popularity, and in other respects. They range from the almost obvious (but not necessarily ineffective) to the most creative (not necessarily most effective). In fact, so many methods have been developed like, Perturb and Observe Method (P&O) [6], Incremental Conductance Method (IC) [7], Sliding Mode Control Method [8] that are widely used for MPPT system in PV, and other method like, Constant Voltage (CV) [9], Short-current Pulse Method [10], Open Voltage Method [11], Fuzzy Logic Control [12], Neutral Network [13], and other unpopular method is also used in different field of MPPT [6]. Therefore, it has become difficult to adequately determine which method, newly proposed or existing is most appropriate for a given PV system.

In this research, the P&O method is selected as the model design in MPPT because its algorithm is easily to implement with both analog and digital implementation by comparing with other method [5]. P&O start perturbing periodically by incrementing, or decrementing the PV output voltage and comparing the PV output power with those of the previous perturbation cycle. Figure 2-18 is the P&O flowchart where P&O algorithm tracks the PV operating point in that direction if the PV output voltage and power increases ($dP/dV > 0$). Otherwise, the operating point is tracked in the opposite direction. The algorithm continues in the same way in the next perturbation cycle.

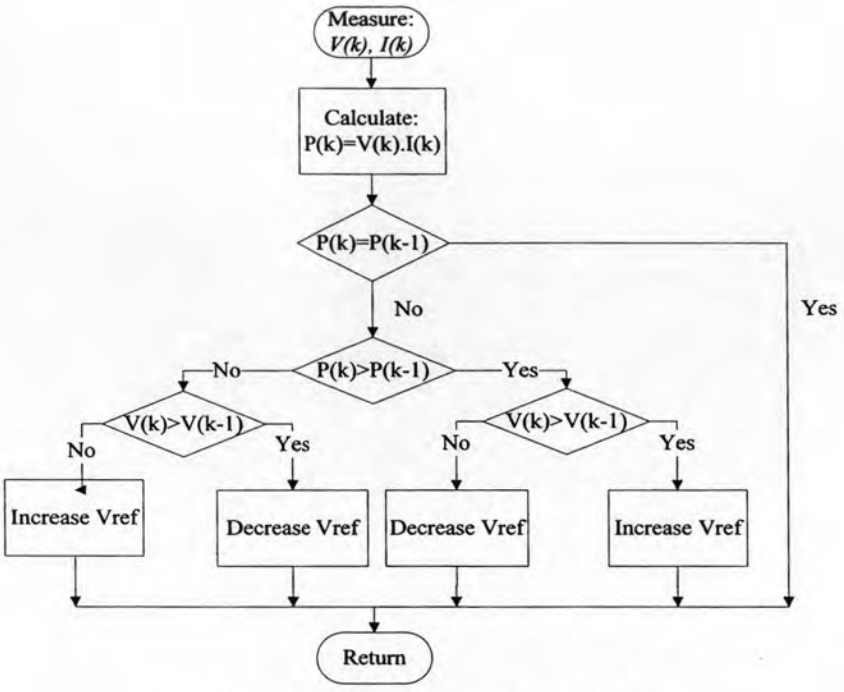

Figure 2-18 P&O MPPT flowchart

2.3.3 PWM Inverter [4]

In order to understand the concept of inverter PWM, first the discussion of PWM with full-bride dc-dc converter is highlighted and the inverter circuits will be clarified thereafter. In PWM of full-bride dc-dc converter, there exists the control signal $v_{control}$ (constant or slowly varying in time) was compared with a repetitive switching-frequency triangular wave form in order to generate switching signals. And the controlling the switch duty ratios allowed the average dc voltage output to be controlled.

In the full-bride converter shown in figure 2-19 [4], the input is fixed-magnitude dc voltage, V_d. The output of the converter is a dc voltage, V_0 which can be controlled in magnitude as well as polarity. In the bipolar voltage switching type, switches (T_{A^+}, T_{B^-}) and (T_{B^+}, T_{A^-}) are treated as switch pairs (two switches in a pair are simultaneously turned on and off). The switching signals are generated by comparing switching-frequency triangular waveforms v_{tri} with control voltage $v_{control}$. When $v_{control} > v_{tri}$, T_{A^+} and T_{B^-} are turned on.

The switch duty ratios can be obtained from the waveforms in figure 2-20 [4] as follows by arbitrary choosing a time origin as shown in the figure:

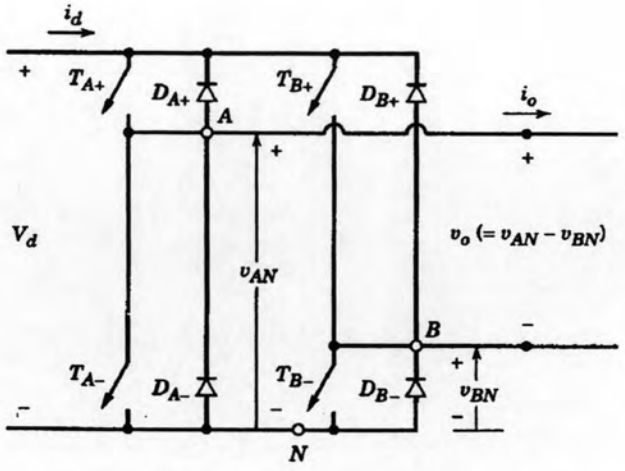

Figure 2-19 Full-bridge dc-dc converter

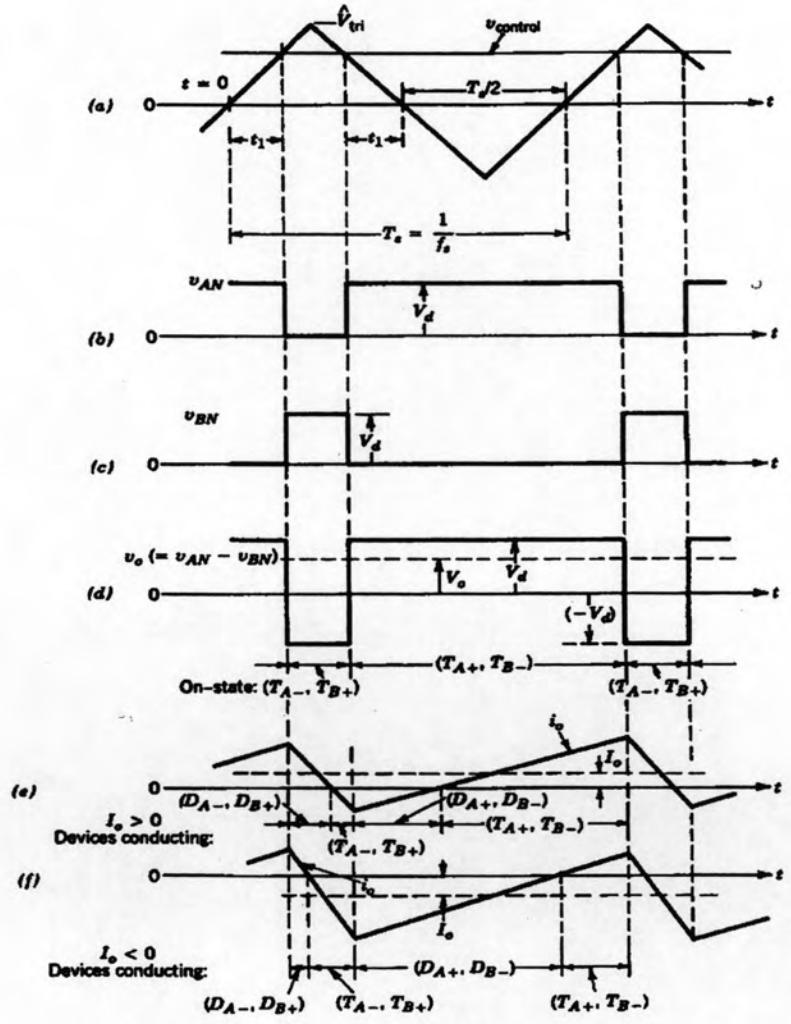

Figure 2-20 PWM with bipolar voltage switching

$$v_{tri} = \hat{V}_{tri}\frac{t}{T_s/4} \qquad 0 < t < \frac{1}{4}T_s \tag{2-19}$$

From equation 2-19, at $t = t_1$ and $v_{tri} = v_{control}$ shown in figure 2-20.a, so:

$$t_1 = \frac{v_{contol}}{\hat{V}_{tri}}\frac{T_s}{4} \tag{2-20}$$

From figure 2-20.a, we also fine that the on duration of switch pair 1 (T_{A+}, T_{B-}) is:

$$t_{on} = 2t_1 + \frac{1}{2}T_s \tag{2-21}$$

Therefore, their duty ratio defined as:

$$D_1 = \frac{t_{on}}{T_s} = \frac{1}{2}\left(1 + \frac{v_{control}}{\hat{V}_{tri}}\right) \tag{2-22}$$

And the duty ratio D_2 of the switch pair 2 (T_{B+}, T_{A-}) is:

$$D_2 = 1 - D_1 \tag{2-23}$$

By using these duty ratio, from figure 2-20.d we can obtain $V_{AN}, V_{BN}, and\ V_0$:

$$V_0 = V_{AN} - V_{BN} = D_1V_d - D_2V_d = (2D_1 - 1)V_d \tag{2-24}$$

Substituting D_1 from equation 2-22 into equation 2-24 yields

$$V_0 = \frac{V_d}{\hat{V}_{tri}}v_{control} \tag{2-25}$$

The basic of switching-mode for dc-to-ac inverter is derived from the one-leg inverter as shown in figure 2-21 [4] and it will assume that the midpoint "o" of the dc input voltage is available. Unlike PWM of full-bride dc-dc converter, in the case of inverter circuit, the PWM is bit more complex, since we would like the invert output to be sinusoidal with magnitude and frequency controllable. In order to produce a sinusoidal output voltage waveform at a desired frequency, a sinusoidal control signal at a desired frequency is compared with a triangle wave form as shown in figure 2-22. The output voltage v_{Ao} fluctuates between two values $\left(\frac{1}{2}V_d\ and\ -\frac{1}{2}V_d\right)$.

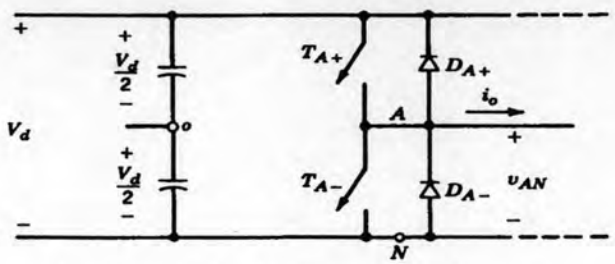

Figure 2-21 One-leg switch-mode inverter

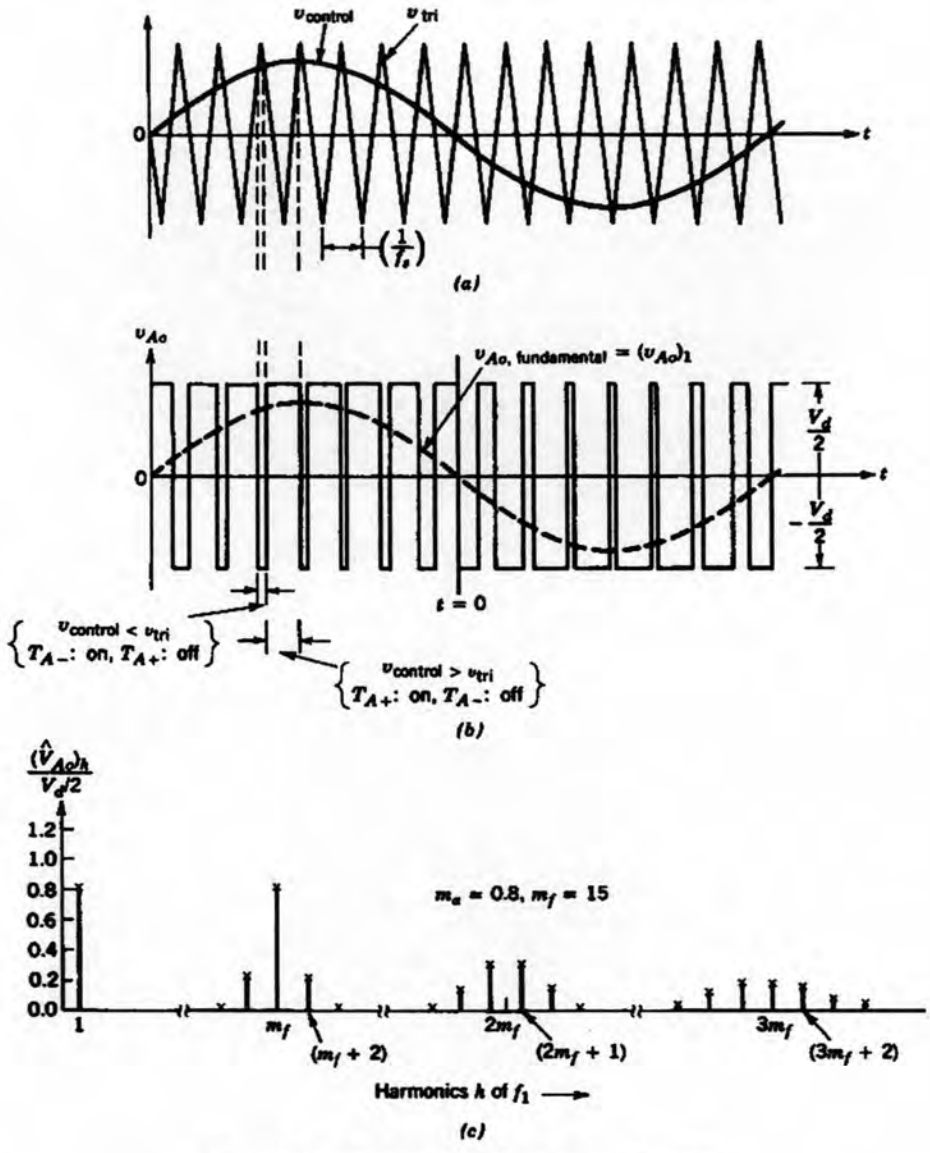

Figure 2-22 Pulse-width modulation (PWM)

Considering a constant $v_{control}$ as shown in figure 2-22.a and from the aforementioned PWM in a full-bride dc-dc converter, the output voltage averaged over one switching time period $T_s = 1/f_s$ is given as follows:

$$V_{Ao} = \frac{v_{control}}{\hat{V}_{tri}} \frac{V_d}{2} \tag{2-26}$$

Assuming that $v_{control}$ varies very little during a switching time period, that is, $m_f = \frac{f_s}{f_1}$ is large, as shown in figure 2-22.b, therefore, assuming $v_{control}$ to be constant over a switching time period, equation 2-25 indicate how the "instantaneous average" value of v_{Ao} (averaged over one switching time period T_s) varies from one

switching time period to the next. This "instantaneous average" is the same as fundamental-frequency component of v_{Ao}.

The foregoing argument shows why $v_{control}$ is chosen to be sinusoidal to provide a sinusoidal output voltage shown in figure 2-23.

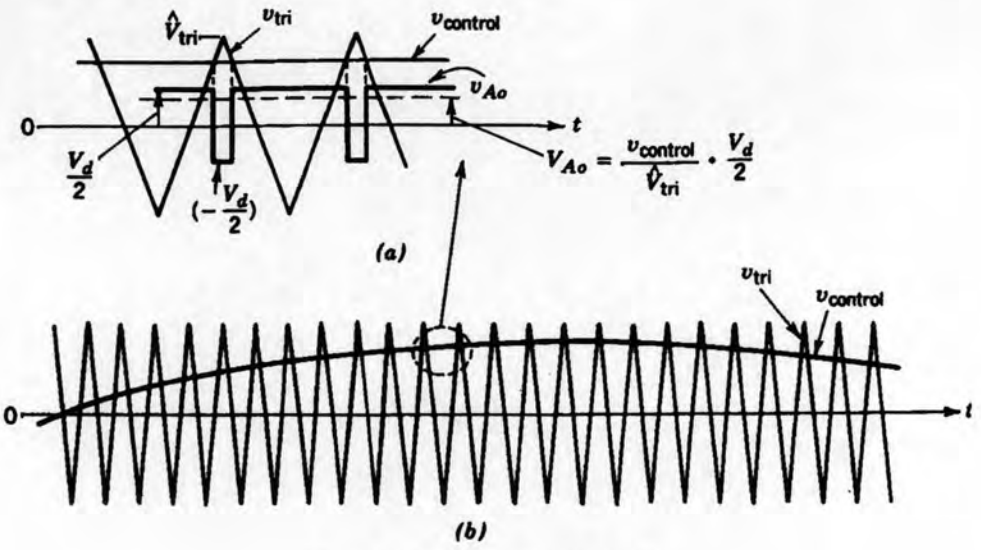

Figure 2-23 Sinusoidal PWM

And let the control voltage vary sinusoidally at the frequency $f_1 = \omega_1/2\pi$, which is the desired (or fundamental) frequency of the inverter output:

$$v_{control} = \hat{V}_{control} \sin \omega_1 t \quad \hat{V}_{control} \leq \hat{V}_{tri} \tag{2-27}$$

Using equation 2-26 and 2-27, the fundamental-frequency component $(v_{Ao})_1$ varies sinusoidally and in phase with $v_{control}$ as a function of time, result in

$$(v_{Ao})_1 = \frac{\hat{V}_{control}}{\hat{V}_{tri}} \sin \omega_1 t \frac{V_d}{2} = m_a \sin \omega_1 t \frac{V_d}{2} \tag{2-28}$$

Therefore,

$$(\hat{V}_{Ao})_1 = m_a \frac{V_d}{2} \tag{2-29}$$

Similarly, the three phase inverters also use PWM to shape and control the three phase output voltages in magnitude and frequency with constant input voltage V_d. In order to get the balanced three phase output voltage, the same triangle voltage waveform is compared with three sinusoidal control voltages that are 120° phase shift as shown in figure 2.24.a [4]. Figure 2-24.b illustrates the line-to-line voltages, for

example V_{AB} that comes from the cancellation between dc components, V_{AN} and V_{BN}. The harmonics in line-to-line voltage are of concern shown in figure 2.24.c because of the 120° phase shift with the odd m_f that could eliminate even harmonics.

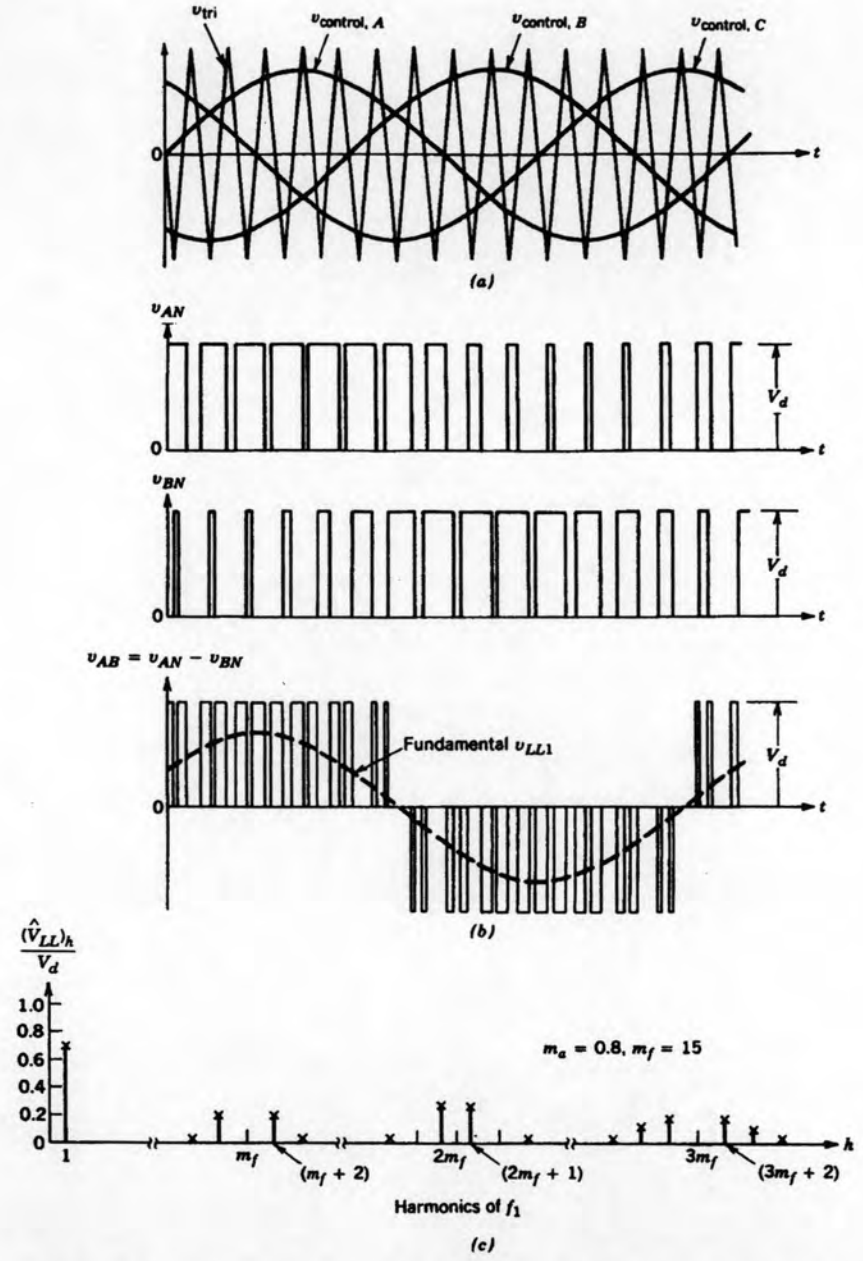

Figure 2-24 Three-phase PWM waveforms and harmonic spectrum

Therefore, the line-to-line rms voltage at the fundamental frequency can be derived:

$$V_{LL_1} = \frac{\sqrt{3}}{\sqrt{2}}(\hat{V}_{AN})_1 = \frac{\sqrt{3}}{2\sqrt{2}} m_a V_d \simeq 0.612 m_a V_d \qquad \textbf{(2-30)}$$

2.3.4 Voltage Regulator

The load voltage is regulated by a PI voltage regulator shown in figure 2-25 using abc_to_dq0 and dq0_to_abc transformations [14]. In this control, the output voltage of PV after the inverter, V_{abc}, is transformed via a time dependent transformation which used abc_to_dq0 transformation in equation 2-31 because it needs to get the low frequency control signals and rapid calculation where it is assuming that the high frequency term is filtered out by the LC filter. The $V_d(t)$, $V_q(t)$ are used to compare with its reference values in p.u, $V_{d,ref}(t)$, $V_{q,ref}(t)$ in order to find the error value, $V_{dq,err}$. The proportional plus integral (PI) is used to minimize the error from $V_{dq,err}$. Then it is transformed back into V_{abc} by dq0_to_abc as shown in equation 2-32. Finally it is used to drive PWM signal that control the inverter.

$$\begin{bmatrix} V_d(t) \\ V_q(t) \\ V_0(t) \end{bmatrix} = \frac{2}{3} \begin{bmatrix} \cos(\omega_e t) & \cos(\omega_e t - \frac{2\pi}{3}) & \cos(\omega_e t + \frac{2\pi}{3}) \\ -\sin(\omega_e t) & -\sin(\omega_e t - \frac{2\pi}{3}) & -\sin(\omega_e t + \frac{2\pi}{3}) \\ \frac{1}{2} & \frac{1}{2} & \frac{1}{2} \end{bmatrix} \begin{bmatrix} V_{an}(t) \\ V_{bn}(t) \\ V_{cn}(t) \end{bmatrix} \quad \textbf{(2-31)}$$

$$\begin{bmatrix} V_a(t) \\ V_b(t) \\ V_c(t) \end{bmatrix} = \begin{bmatrix} \cos(\omega_e t) & -\sin(\omega_e t) & 1 \\ \cos(\omega_e t - \frac{2\pi}{3}) & -\sin(\omega_e t - \frac{2\pi}{3}) & 1 \\ \cos(\omega_e t + \frac{2\pi}{3}) & -\sin(\omega_e t + \frac{2\pi}{3}) & 1 \end{bmatrix} \begin{bmatrix} V_d(t) \\ V_q(t) \\ V_0(t) \end{bmatrix} \quad \textbf{(2-32)}$$

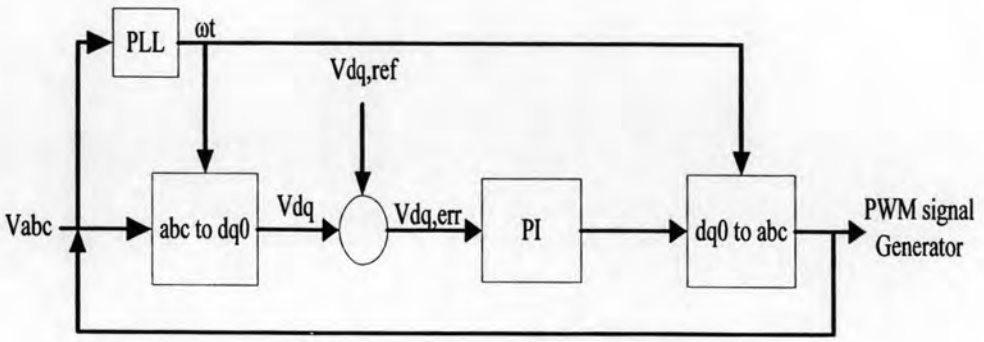

Figure 2-25 Voltage regulator diagram

2.4 Synchronous Machine Distributed Generation [15]

The synchronous machine distributed generation (SG) is a device that converters mechanical power from a prime mover to alternative electric power at a specific frequency and voltage. SG has been used throughout the world to produce the vast majority of electric power. Generally, SG can operate as generator mode if the mechanical power is positive, and it will operate as motor mode if the mechanical power is negative. The electrical system for each phase consists of a voltage source in series with RL impedance, which implements the internal impedance of the machine. The mechanical system of SG derived as:

$$\Delta\omega(t) = \frac{1}{2H}\int_0^t (T_m - T_e)dt - K_d\Delta\omega(t) \quad \textbf{(2-33)}$$

$$\omega(t) = \Delta\omega(t) + \omega_0 \quad \textbf{(2-34)}$$

where $\Delta\omega$: Speed variation with respect to speed of operation

H: Constant of inertia

T_m: Mechanical torque

T_e: Electromagnetic torque

K_d: Damping factor representing the effect of damper windings

$\omega(t)$: Mechanical speed of the rotor

ω_0 : Speed of the operation

The K_d damping coefficient simulates the effect of damper windings normally used in synchronous machines. When the machine is connected to an infinite network (zero impedance), the variation of machine power angle delta (δ) resulting from a change of mechanical power (P_m) can be approximated by the following second-order transfer function:

$$\frac{\delta}{P_m} = \frac{\omega_s / 2H}{s^2 + 2\varsigma\omega_n s + \omega_n^2} \quad \textbf{(2-35)}$$

$$\omega_n = \sqrt{\omega_s . P_{\max} / 2H} \quad \textbf{(2-36)}$$

$$\varsigma = (K_d / 4).\sqrt{2 / (\omega_s.P_{\max}.H)} \quad \textbf{(2-37)}$$

$$P_{\max} = V_t.E / X \quad \textbf{(2-38)}$$

$$K_d = 4\varsigma\sqrt{\omega_s.H.P_{\max} / 2} \quad \textbf{(2-39)}$$

where δ : Power angle (rad/s)

P_m: Mechanical power

ω_n :Frequency of electromechanical oscillation (rad/s)

ω_n : Electrical frequency (rad/s)

P_{max}: Maximum power transmitted through reactance X at terminal voltage V_t and internal voltage E

H: Inertia constant (s)

K_d: Damping factor

The SG model taken from the MATHLAB-SIMULINK that will be used in the study cases in this research is shown in figure 2-26. There are two kind of SG models, like synchronous machine SI unit, and synchronous machine p.u unit. Its different is just only the input parameter where model in SI required the exact value input, for example Vf=22kV whereas the model p.u required only the per unit value like Vf=1 p.u. Their input parameters block of the SG model is detail in appendix A

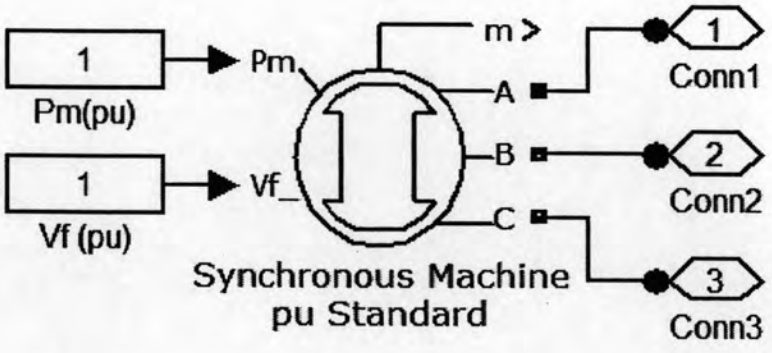

Figure 2-26 Synchronous machine in MATLAB-SIMULINK